Available online at www.sciencedirect.com
SCIENCE DIRECT®
International Journal of Heat and Mass Transfer 48 (2005) 171–181
International Journal of HEAT and MASS TRANSFER
www.elsevier.com/locate/ijhmt

An analysis of entropy generation through a circular duct with different shaped longitudinal fins for laminar flow

İhsan Dağtekin [a], Hakan F. Öztop [a,*], Ahmet Z. Şahin [b]

[a] Department of Mechanical Engineering, Firat University, 23119 Elazig, Turkey
[b] Department of Mechanical Engineering, King Fahd University of Petroleum and Minerals, Dhahran 31261, Saudi Arabia

Received 30 January 2004

Abstract

The present study focuses on the entropy generation analysis in a circular duct with internal longitudinal fins of different shape for laminar flow. Three different fin shapes are chosen for the analysis: Thin, triangular and V-shaped fins. Calculations are performed for various dimensionless lengths and number of fins, dimensionless temperature difference and fin angle for triangular and V-shaped fins. It is found that the number of fins and dimensionless length of the fins for both thin fins and triangular fins, and the fin angle for triangular and V-shaped fins have significant effect on both entropy generation and pumping power. Further, both entropy generation and pumping power also are influenced by dimensionless temperature difference.

Keywords: Entropy generation; Laminar flow; Circular duct; Longitudinal fins

1. Introduction

Pipes with internal or external longitudinal fins are used to enhance heat transfer as a passive method. The heat transfer across the stream to stream ΔT and the frictional ΔP experienced by each stream represent two different facets of one single aspect of the heat exchanger, namely, its degree of thermodynamic irreversibility [1]. From this point of view, the second law analysis is used to determine the optimum heat exchanger dimensions. Ducts with longitudinal fins of different shapes are also widely used in compact heat exchanger applications [2–5]. Such geometries are called internally finned tubes.

Bejan [6] investigated the concept of irreversibility for heat exchanger design in counter-flow heat exchangers. He illustrated a design approach for a heat exchanger by using the second law analysis of thermodynamics. It was found that the entropy generation unit method is more useful than the traditional heat exchanger design technique. In his another study, he obtained the entropy generation in fundamental convective heat transfer problems and provided some examples [7].

Sahin [8] made an analytical study of the second law analysis for laminar viscous flow through a duct subjected to constant wall temperature. It was found that entropy generation, ψ, increases with increasing the dimensionless temperature difference. However, pumping power ratio decreases with increasing temperature

* Corresponding author: Tel.: +90 424 2370 000x6331; fax: +90 424 2415 526.
E-mail address: hfoztop@hotmail.com (H.F. Öztop).

0017-9310/$ - see front matter © 2004 Elsevier Ltd. All rights reserved.
doi:10.1016/j.ijheatmasstransfer.2004.08.013

Nomenclature

A	cross-sectional area of duct (m^2)
C_p	specific heat capacity (J/kg K)
D	diameter of pipe
D_H	hydraulic diameter (m)
d	radius of tube
f	friction factor
$\bar{h}$	average heat transfer coefficient ($W/m^2 K$)
k	thermal conductivity (W/m K)
L	length of duct (m)
L_d	fin length (m)
L^*	non-dimensional fin length for thin fin, L/d
L_u^*	non-dimensional fin length for triangular fin, L/d
L_v^*	non-dimensional fin length for V-shaped fin, L/L_{max}
L_{max}	defined in Eq. (6)
m	mass flowrate (kg/s)
n	number of fins
$\overline{Nu}$	average Nusselt number (hD_H/k)
p	perimeter of duct (m)
P	pressure (N/m^2)
PPR	pumping power to heat transfer ratio ($A\Delta P\overline{U}/\dot{Q}$)
Pr	Prandtl number ($\mu C_p/K$)
$\dot{Q}$	total heat flux (W)
Re	Reynolds number ($\rho\overline{U}D_H/\mu$)
s	entropy (J/kg K)
$\dot{S}_{gen}$	entropy generation (W/K)
St	Stanton number $\bar{h}/(\rho\overline{U}C_p)$
T	temperature (K)
T_0	inlet fluid temperature (K)
T_w	wall temperature of the duct (K)
$\overline{U}$	fluid bulk velocity (m/s)
x	axial distance (m)
ΔP	total pressure drop (N/m^2)
ΔT	increase of fluid bulk temperature (K)
μ	viscosity ($N s/m^2$)
λ	non-dimensional axial distance (L/D_H)
Π_1	non-dimensional group ($4\overline{Nu}\lambda/Pr$)
Π_2	non-dimensional group $(\mu^2\lambda(fRe)/(2\rho^2 D_H^2 C_p T_w))$
ψ	non-dimensional entropy generation
ρ	density (kg/m^3)
τ	non-dimensional inlet wall-to-fluid temperature difference $((T_0 - T_w)/T_w)$
ϕ	fin angle

difference. In the case of small value of the dimensionless temperature difference, the entropy generation due to viscous friction becomes dominant. For constant wall temperature condition, a thermodynamic optimization was performed by Nag and Mukherjee [9]. They observed that the initial temperature difference between fluid and the wall is an important design criterion. Entropy generation for a duct under constant heat flux boundary conditions was analyzed by Sahin [10]. For low heat flux boundary condition, it was found that the entropy generation due to viscous friction is dominant. Hydraulic diameter of the duct is found to be an effective parameter as a design criterion for second law analysis on both constant wall heat flux and constant wall temperature boundary conditions. In both cases, it is found that circular duct is the most feasible geometry.

A number of numerical and experimental studies on ducts with longitudinal fins can be found in the literature from the point of view of flow field and heat transfer rates. Due to space limitation in this paper only a few of them are mentioned here. Fabbri [11] made a numerical study by using a finite element code to solve optimization problem in a duct with longitudinal convective fins of both symmetrical and asymmetrical position. It was shown some optimized geometries and found that under particular conditions, noticeable improvements in the heat transfer have been observed for optimum fins with asymmetrical polynomial lateral profiles. In another study, the same author investigated the optimum internal fins of asymmetric shape in a circular tube [12,13]. Fins of polynomial shape have been used to enhance heat transfer in circular tube configuration. Ifhakhar and Ghoshdastidar [14] made a numerical study to solve heat transfer and fluid flow in circular tubes with internal longitudinal fins having tapered lateral profiles for laminar flow conditions. Braga and Saboya [15] performed an experimental study to determine average heat transfer coefficients and friction factors for turbulent flow through annular ducts with continuous longitudinal rectangular fins. Average Nusselt number and friction factor as functions of flow Reynolds number were obtained. Kumar [16] made a numerical study to obtain natural convection heat transfer rates and flow fields in a vertical annulus with longitudinal fins with various parameters. It was found that the heat transfer rates increase as the fin ratio and radius ratio increase. In addition, the heat transfer rates decrease if the aspect ratio and the fin thickness angle increase. Zeitoun and Hegazy [17] solved numerically the momentum and the energy equations to obtain heat transfer augmentation in laminar flow for internal longitudinal thick fins. Their study showed that the results obtained for different pipe-fin geometries show that the fin heights affect greatly the

flow and the heat transfer characteristics. Reducing the height of one fin group decreases the friction coefficient significantly. At the same time Nusselt number decreases inappreciably so that such reduction is justified. Yu et al. [18] made an experimental study for internal wave-like longitudinal fins to investigate heat transfer augmentation and pressure drop in a double pipe. They used two cases. In the first case, blocked annular pipe is used, and the second one is unblocked. They found that wave-like fins enhance heat transfer significantly with the blocked case being superior. Campo and Chang [19] performed an analytical study to obtain some correlation for friction factors and convective coefficients in internal longitudinal tubular heat exchanger. Empirical correlation equations are applicable for the asymptotic friction factor and the asymptotic Nusselt numbers as functions of the number of fins and the relative fin height in the bundle.

The objective of this paper is to discuss the entropy generation and the pumping power variations in a circular duct with longitudinal thin, triangular and V-shaped fins respectively, for laminar flow and constant wall temperature conditions. To best knowledge of the authors, this subject has not been addressed in the literature and the present study is considered as a first attempt in this context.

2. The physical models

This study was performed for three different cases: a circular duct with thin longitudinal fins, a circular duct with triangular fins and a circular duct with V-shaped fins respectively, as shown in Fig. 1a–c. The length of circular duct was considered to be long enough such that the flow in the duct can be assumed to be hydrodynamically developed. For the geometrical parameters, necessary calculations can be given as follows.

The hydraulic diameter, D_H, of the circular duct with thin longitudinal fins shown in Fig. 1a (for the fin thickness treated as zero), is given by

$$D_H = \frac{\pi d^2}{\pi d + 2nL_d} \tag{1}$$

where d is the diameter of the duct, L is the height of fins and n is the number of fins.

For the longitudinal triangular fin geometry (Fig. 1b), the hydraulic diameter D_H is given as

$$D_H = 4\left(\frac{A_c}{P}\right) \tag{2}$$

where

$$A_c = \pi d^2 - n[d^2\phi - d(d - L_d)\sin\phi] \tag{3}$$

$$p = 2\pi d + 2nL' - 2n\phi d \tag{4}$$

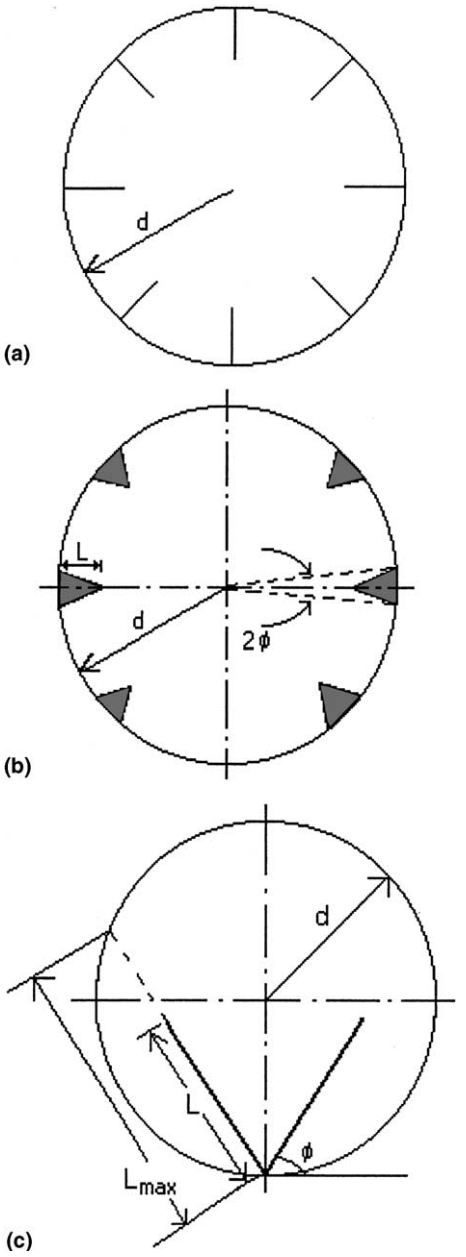

Fig. 1. A circular duct with (a) longitudinal thin fins, (b) triangular longitudinal fins and (c) V-shaped longitudinal fins.

$$L' = \left[d^2 + (d - L_d)^2 - 2d(d - L_d)\cos\phi\right]^{1/2} \tag{5}$$

with the fin angle and L the height of the triangular cross-section, as shown in Fig. 1b. For the V-shaped longitudinal fins, the hydraulic diameter can be expressed as:

$$D_H = \frac{2d}{1 + (2L_d/\pi d)}, \quad L_{max} = 2\sin\phi \tag{6}$$

where L is the height of the fins, as shown in Fig. 1c.

3. Analysis

Water is considered as a working fluid in the analysis. Thermophysical properties of the fluid are assumed constant and they are listed in Table 1. The mean Nusselt number and (fRe) values were obtained from the experimental studies available in the literature for different geometrical parameters [3] and they are tabulated in Tables 2–4. For given geometries, the Nusselt number does not depend on the thermal conductivity of the fin material since it is associated to an ideal isothermal fin, that is, its efficiency was considered as 100% [13,3]. The inlet temperature T_0 is assumed to be uniform at the inlet of the duct. No-slip condition is applied along the duct wall and fin surfaces for the flow and laminar fully developed flow regime is also assumed. Using these assumptions, the heat transfer for an incompressible flow in an infinitesimal control volume of thickness dx in the duct can be written as

$$\delta\dot{Q} = \dot{m}C_p\,\mathrm{d}T = \bar{h}p(T_\mathrm{w} - T)\,\mathrm{d}x \tag{7}$$

where the mass flow rate is given by

$$\dot{m} = \rho\overline{U}A \tag{8}$$

The entropy generation for this control volume can be written as

Table 1
Thermo physical properties of water [18]

	Water
C_p (J/kg K)	4182
Pr	7
T_w (K)	293
μ (N s/m^2)	9.93×10^{-4}
ρ (kg/m^3)	998.2

Table 2
Nusselt number values for circular duct with longitudinal thin fins [3]

n	$L^*=0.2$	0.4	0.6	0.7	0.8	0.9	1.0
Nusselt number values							
4	4.58	6.05	11.82	15.34	19.30	–	19.08
8	4.74	6.98	21.10	34.27	42.58	–	40.68
12	4.77	6.65	20.52	40.92	72.27	–	68.80
16	4.74	6.09	16.22	34.45	106.50	105	103.4
20	4.68	5.64	12.73	26.07	138.35	147.20	144.6
24	4.62	5.32	10.41	19.83	156.92	195.40	192.4
fRe							
4	19.13	29.04	50.31	59.31	73.43	–	77.26
8	22.39	47.02	110.81	137.35	170.47	–	175.96
12	25.55	64.22	179.77	233.09	303.16	–	314.99
16	28.20	77.86	246.08	336.15	469.92	491.04	495.24
20	30.33	88.04	305.47	439.13	668.23	708.29	716.79
24	32.01	95.57	356.04	537.09	894.15	965.09	980.77

Table 3
Nusselt number values for circular duct with longitudinal triangular fins [3]

n	$L^*=0.2$	0.4	0.6	0.7	0.8
Nusselt numbers for $2\phi=3°$					
4	4.58	6.03	11.72	18.02	19.29
8	4.73	6.85	20.01	43.26	43.60
12	4.75	6.42	17.82	64.58	76.17
16	4.71	5.82	13.15	63.21	112.11
20	4.64	5.37	9.95	46.17	131.9
24	4.58	5.07	8.02	30.86	117.5
fRe for $2\phi=3°$					
4	19.20	29.35	51.73	69.56	77.24
8	22.56	48.16	118.4	174.2	194.2
12	25.78	66.13	198.3	326.3	376.7
16	28.50	80.36	277.4	523.5	638.1
20	30.61	90.66	348.0	759.4	990.2
24	32.26	98.15	407.3	1021.8	1440.5
Nusselt numbers for $2\phi=6°$					
4	4.58	4	4.58	4	4.58
8	4.71	8	4.71	8	4.71
12	4.73	12	4.73	12	4.73
16	4.67	16	4.67	16	4.67
20	4.6	20	4.6	20	4.6
24	4.54	24	4.54	24	4.54
fRe for $2\phi=6°$					
4	19.29	29.74	53.25	71.91	81.41
8	22.77	49.38	126.9	193.0	223.4
12	26.09	68.25	219.2	388.5	479.4
16	28.86	82.79	311.8	665.5	903.8
20	31.02	93.25	392.7	1013.3	1560.9
24	32.65	100.6	456.8	1402.2	2502.2

$$\mathrm{d}\dot{S}_\mathrm{gen} = \dot{m}\,\mathrm{d}s - \frac{\delta\dot{Q}}{T_\mathrm{w}} \tag{9}$$

where for an incompressible fluid,

$$\mathrm{d}s = C_p\frac{\mathrm{d}T}{T} \tag{10}$$

Substituting Eqs. (7) and (10) into Eq. (9), the total entropy generation recasts as,

$$\mathrm{d}\dot{S}_\mathrm{gen} = \dot{m}C_p\frac{T_\mathrm{w}-T}{TT_\mathrm{w}}\mathrm{d}T \tag{11}$$

Integrating Eq. (7) over the finite length of duct of L_d, the bulk temperature variation of the fluid and the total heat transfer along the duct can be obtained [20], respectively, as:

$$T = T_\mathrm{w} - (T_\mathrm{w} - T_0)\exp\left(-\frac{4\bar{h}}{\rho\overline{U}D_\mathrm{H}C_p}X\right) \tag{12}$$

$$\dot{Q} = \dot{m}C_p(T_\mathrm{w} - T_0)\left[1 - \exp\left(-\frac{4\bar{h}L_\mathrm{d}}{\rho\overline{U}D_\mathrm{H}C_p}\right)\right] \tag{13}$$

A non-dimensional total entropy generation can be defined based on the flow stream capacity rate ($\dot{m}C_p$) as

Table 4
Nusselt number values for circular duct with longitudinal V-shaped fins [3]

ϕ	$L_1^* = L/L_{max}$	Nu	fRe
30	0.2	4.359	16.353
	0.4	4.386	17.059
	0.6	4.400	17.776
	0.8	4.403	18.203
40	0.2	4.385	16.799
	0.4	4.472	18.567
	0.6	4.535	20.497
	0.8	4.521	21.731
50	0.2	4.426	17.444
	0.4	4.681	21.034
	0.6	4.895	25.735
	0.8	4.887	29.046
60	0.2	4.496	18.154
	0.4	5.071	24.351
	0.6	5.994	34.527
	0.8	6.376	43.552
65	0.4	5.341	26.022
	0.6	7.209	39.903
	0.8	8.703	54.368
67.5	0.4	5.501	26.724
	0.6	7.990	42.620
	0.8	10.885	60.129
70	0.4	5.647	27.328
	0.6	8.856	45.009
	0.8	13.981	65.356
72.5	0.4	5.768	27.810
	0.6	9.771	46.607
	0.8	17.218	69.095
75	0.4	5.872	28.072
	0.6	10.469	47.342
	0.8	18.01	70.942
77.5	0.6	10.787	47.078
	0.8	16.353	69.702
80	0.6	10.477	46.070
	0.8	13.967	65.779

$$\Psi = \frac{\dot{S}_{gen}}{\dot{m}C_p} = \frac{\dot{S}_{gen}}{(\dot{Q}/\Delta T)} \tag{14}$$

On integrating Eq. (11) over the fluid control volume and using Eqs. (12) and (13), the non-dimensional total entropy generation is obtained as

$$\Psi = \ln\left(\frac{1+\tau e^{-4St\lambda}}{1+\tau}\right) + \tau(1-e^{-4St\lambda}) \tag{15}$$

where τ is the non-dimensional temperature difference

$$\tau = \frac{T_0 - T_w}{T_w} \tag{16}$$

λ is the non-dimensional length of duct

$$\lambda = \frac{L_d}{D_H} \tag{17}$$

St is the Stanton number

$$St = \frac{\bar{h}}{\rho \overline{U} C_p} = \frac{\overline{N}u}{RePr} \tag{18}$$

Eq. (15) can be modified and written as a function of the Reynolds number and the other non-dimensional parameters as

$$\Psi = \ln\left(\frac{1+\tau e^{-\Pi_1/Re}}{1+\tau}\right) + \tau(1-e^{-\Pi_1/Re}) \tag{19}$$

where

$$\Pi_1 = 4\frac{\overline{N}u}{Pr}\lambda \tag{20}$$

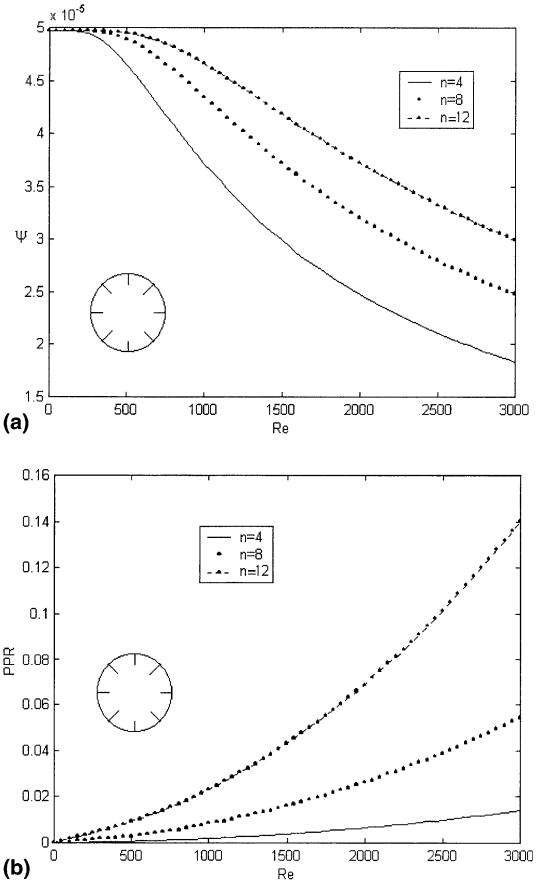

Fig. 2. The effect of fin numbers on (a) entropy generation and (b) pumping power ratio (thin fins, $L^* = 0.4$ and $\tau = 0.01$).

The pumping power to heat transfer ratio (PPR) can be expressed as

$$\mathrm{PPR} = \frac{A\,\Delta P \overline{U}}{\dot{Q}} \tag{21}$$

where ΔP is the total pressure drop which is obtained integrating the value of infinitesimal pressure drop $\mathrm{d}P$ and is related to the friction factor beside other parameters as

$$\mathrm{d}P = -\frac{f\rho\overline{U}^2}{2D_\mathrm{H}}\mathrm{d}x \tag{22}$$

Using Eqs. (13) and (23), the pumping power to heat transfer ratio is obtained as

$$\mathrm{PPR} = \Pi_2 \frac{Re/\tau}{1 - \mathrm{e}^{(-\Pi_1/Re)}} \tag{23}$$

where

$$\Pi_2 = \frac{\mu^2\lambda(fRe)}{2\rho^2 D_\mathrm{H}^2 C_p T_\mathrm{w}} \tag{24}$$

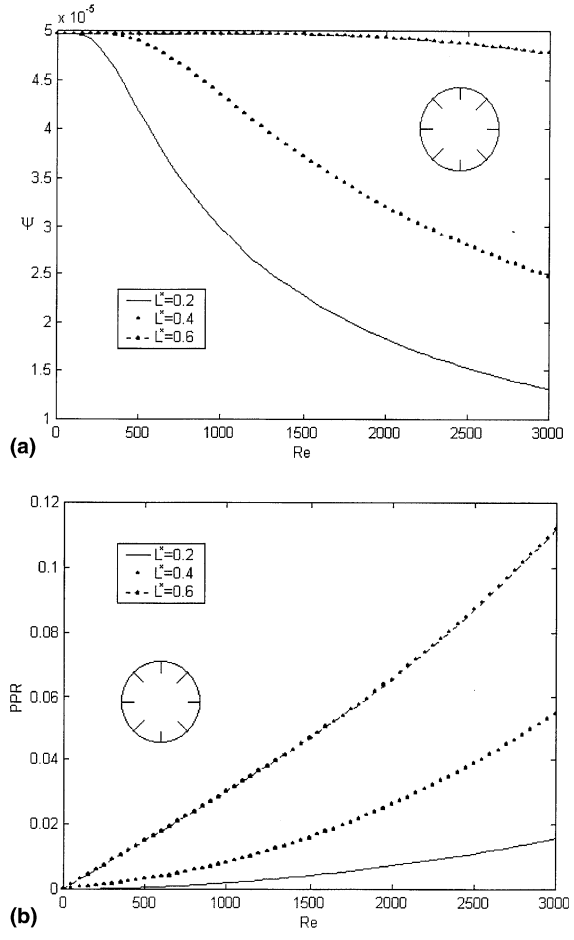

Fig. 3. The effect of fin length on (a) entropy generation and (b) pumping power ratio (thin fins, $n = 8$ and $\tau = 0.01$).

4. Results and discussion

Second law analysis has been carried out for three different duct configuration, namely, circular duct with longitudinal thin fins, longitudinal triangular fins and longitudinal V-shaped fins for laminar flow and under constant wall temperature conditions. Water was used as a working fluid ($Pr = 7$). In the following, the results for each geometry are presented separately. Calculations were performed for different dimensionless temperature difference, τ, and various Reynolds numbers.

4.1. Circular duct with longitudinal thin fins

The effect of thin fins on the dimensionless entropy generation, ψ, and pumping power ratio, PPR, for different Reynolds numbers and dimensionless inlet wall-to-fluid temperature difference, $\tau = 0.01$, is presented in Fig. 2a and b. As it is seen from Fig. 2a, the dimension-

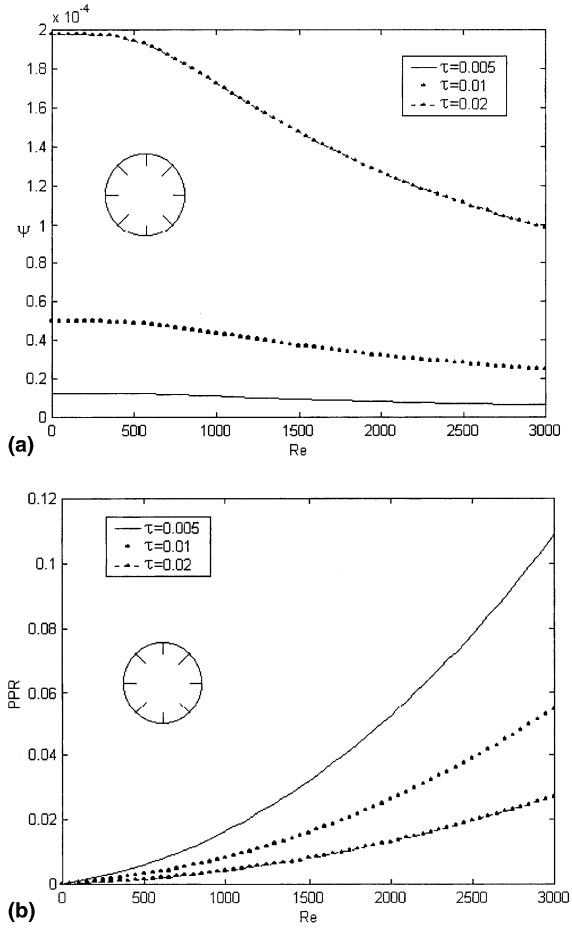

Fig. 4. The effect of dimensionless temperature on (a) entropy generation and (b) pumping power ratio (thin fins, $n = 8$ and $L^* = 0.4$).

less entropy generation decreases exponentially as the Reynolds number increases for a fixed dimensionless fin length of $L^* = 0.4$. For a fixed value of Reynolds number, as the number of fins increase then the dimensionless entropy generation increases. Examining Fig. 2a reveals that, as the number of fins are increased from 4 to 12, the dimensionless entropy generation maintained at the same value for lower Reynolds number of about $Re < 250$. The pumping power to heat transfer ratio variation is indicated in Fig. 2b. As Reynolds number is increased, the contribution due to heat transfer decreases and that of viscous friction increases. Therefore, for low Reynolds number viscous frictional contribution can be neglected. As the number of fins is increased then PPR increases yielding a maximum for $n = 12$. This can be attributed to the Nu number variation with the number of fins, n, that affects the heat transfer directly.

The effect of the length of thin fins on the dimensionless entropy generation, ψ, and the pumping power to heat transfer ratio (PPR) is given in Fig. 3a and b, respectively. In this case, the number of fins is fixed to $n = 8$ and the dimensionless temperature difference is chosen as $\tau = 0.01$. It is clear that, for a fixed Reynolds number the non-dimensional entropy generation increases as the length of fin is increased, but for a chosen fin length value, say $L^* = 0.4$, the non-dimensional entropy generation decreases as Reynolds number is increased, as indicated in Fig. 3a. As the length of fins is increased to maximum value, which becomes equal to radius of the duct the viscous friction increases and gives extremely high ψ values compared to shorter fin lengths. This in turn yields higher non-dimensional entropy generation. In Fig. 3b pumping power ratio variation for different Reynolds numbers is given. As seen from this figure the pumping power ratio value increases as the dimensionless length of fin is increased. For a fixed value, L^* the pumping power ratio increases especially

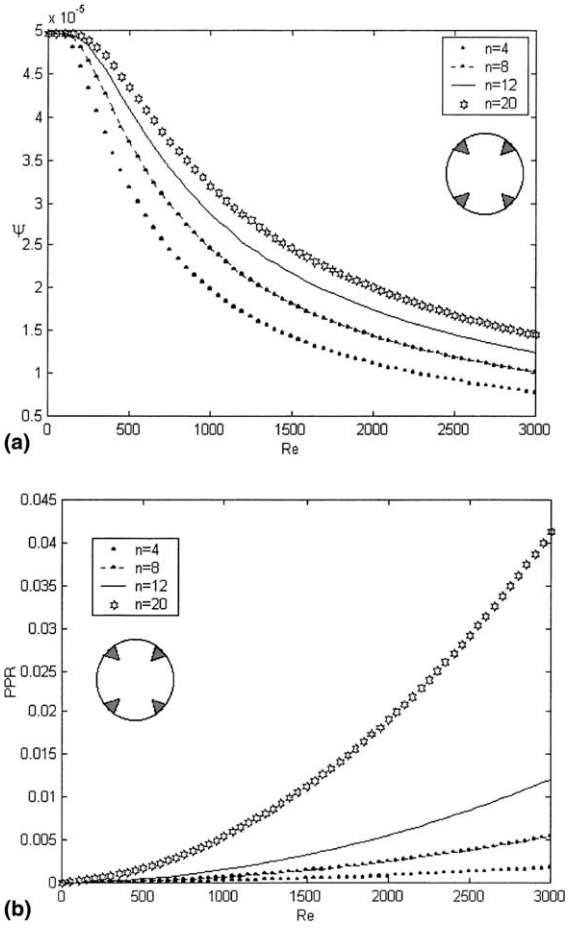

Fig. 5. The effect of fin numbers on (a) entropy generation and (b) pumping power ratio (triangular fin, $L^* = 0.4$, $\tau = 0.01$ and $2\phi = 3°$).

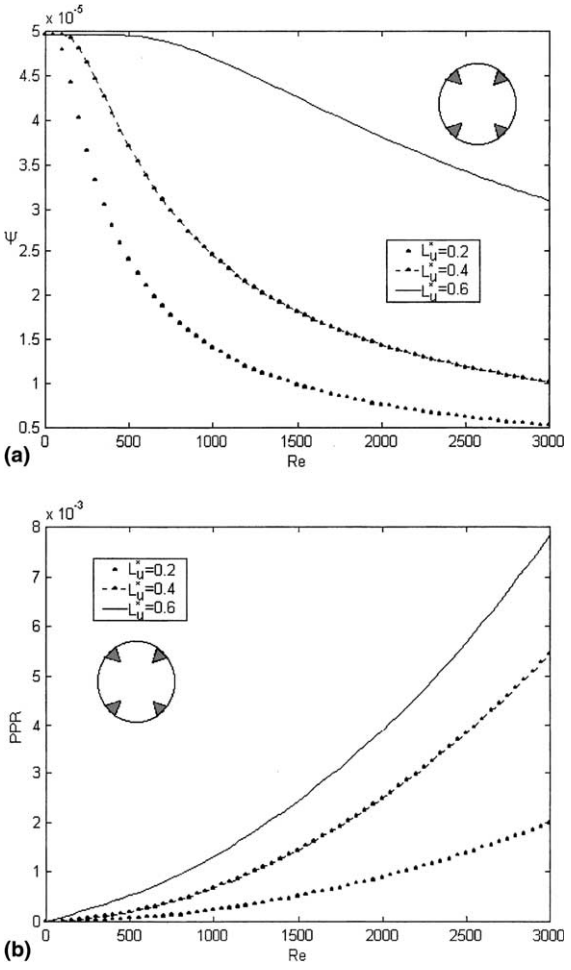

Fig. 6. The effect of fin length on (a) entropy generation and (b) pumping power ratio (triangular fin, $n = 8$, $\tau = 0.01$ and $2\phi = 3°$).

for higher Reynolds number as Reynolds number is increased.

Fig. 4a and b show the effect of dimensionless temperature difference on the dimensionless entropy generation, ψ, and the pumping power to heat transfer ratio for a fixed fin number $n = 8$ and a fixed length of the thin fin $L^* = 0.4$. As seen from Fig. 4a, the dimensionless entropy generation increases with respect to increasing the dimensionless temperature difference τ. As the Reynolds number is increased, the non-dimensional entropy generation decreases but pumping power to heat transfer ratio decreases as seen in Fig. 4a and b. Furthermore, with the increase of dimensionless temperature difference, τ, PPR values decrease as seen in Fig. 4b.

4.2. Circular duct with triangular longitudinal fins

In this section, the effect of triangular fins on the entropy generation and pumping power is analyzed with respect to the geometrical parameters. Fig. 5a shows the effect of the number of triangular fins on the non-dimensional entropy generation. The trend is similar to that obtained for thin fins, namely, as the fin number increases, the dimensionless entropy generation, ψ, is not affected significantly for higher triangular fin numbers ($n > 12$) but the pumping power ratio value increase significantly as observed in Fig. 5b. Figs. 6a and b show the effect of the dimensionless length of triangular fins on the non-dimensional entropy generation and the pumping power to heat transfer ratio for fixed triangular fin angle of $2\phi = 3°$. As can be seen from Fig. 6a, when the length of the triangular fins is increased, the ψ values increase. As the Reynolds number is increased then ψ values decrease showing a similar trend to that obtained for thin fins. Again, higher pumping power ratio values are obtained for higher non-dimensionless fin length (L^*) values. As the Reynolds number increases, the pumping power ratio values increase significantly.

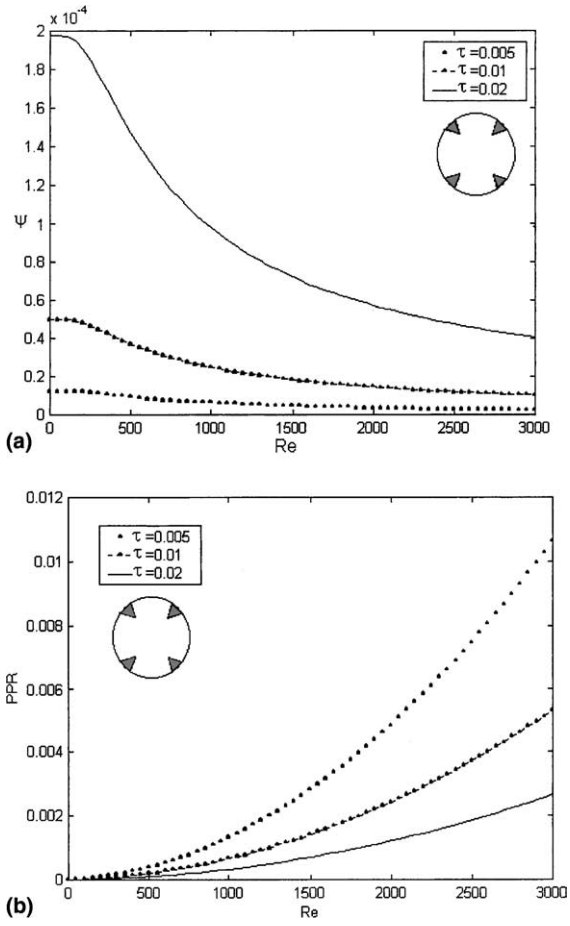

Fig. 7. The effect of dimensionless temperature on (a) entropy generation and (b) pumping power ratio (triangular fins, $n = 8$ and $L^* = 0.4$).

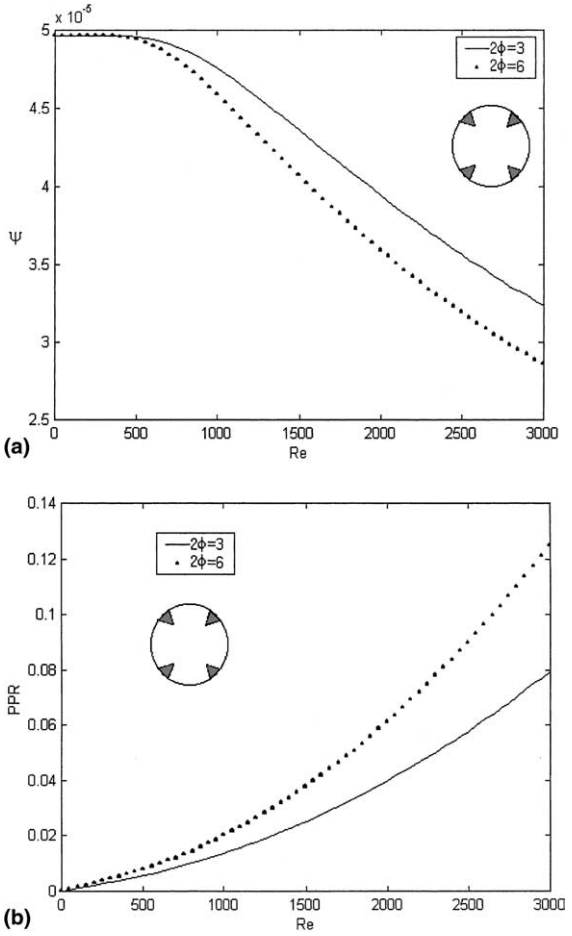

Fig. 8. The effect of fin angle on (a) entropy generation and (b) pumping power ratio (triangular fins, $n = 16$ and $L^* = 0.6$).

The effect of the dimensionless temperature difference on the non-dimensional entropy generation and the pumping power ratio is given in Fig. 7a and b for $n = 8$ and $L^* = 0.4$. As the non-dimensional temperature difference values increase then the non-dimensional entropy generation values increase, while as the Reynolds number increases then the non-dimensional entropy generation values decreases as seen in Fig. 7a. On the other hand pumping power ratio values are high for lower non-dimensional temperature differences.

Another significant parameter in this case is the value of triangular fin angle, 2ϕ. Fig. 8a and b show the effect of angle 2ϕ on the dimensionless entropy generation, ψ, and pumping power to heat transfer ratio, PPR. As it is seen, with the increase of angle of triangle fin dimensionless entropy generation is decreased due to increase of viscous friction. For a fixed fin angle as Reynolds number is increased ψ values decrease dramatically after $Re = 500$ value. On the other hand, with the increase of angle of triangular fin, pumping power to heat transfer ratio increases because hydraulic diameter of the duct becomes smaller, namely cross-section of the duct becomes smaller, Fig. 8b. As cross-section duct is decreased PPR value increases as indicated in Ref. [20].

4.3. Circular duct with longitudinal V-shaped longitudinal fins

The main affecting parameters on this configuration are the angle of fins with respect to horizontal surface, as indicated in Fig. 1c. In order to evaluate the results the dimensionless fin length $L_1^* = L/L_{max}$ is introduced.

Fig. 9a shows the effect of the fin angle on the non-dimensional entropy generation. For higher fin angle values dimensionless entropy generation values become higher. Similar to the configurations discussed above,

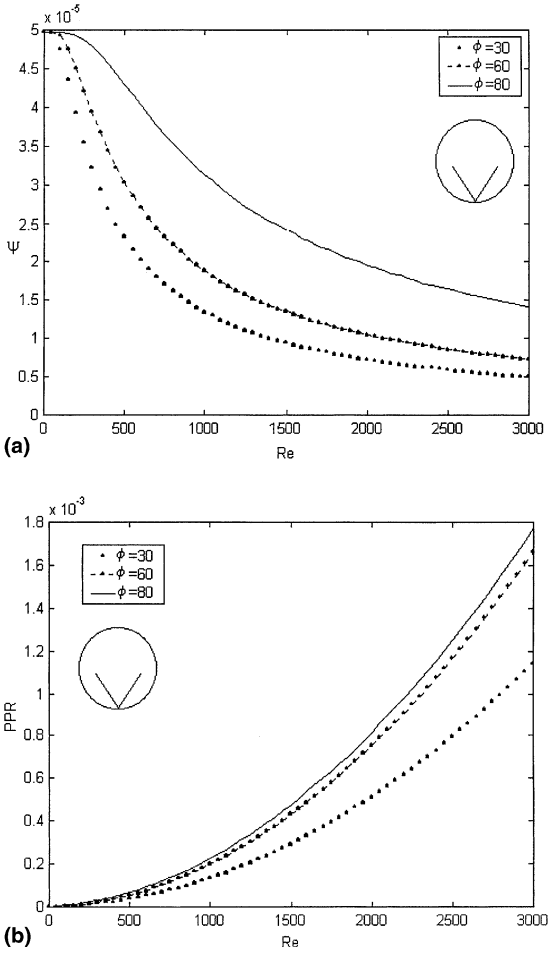

Fig. 9. The effect of fin angle on (a) entropy generation and (b) pumping power ratio (V-shaped fin, $L/L_{max} = 0.6$ and $\tau = 0.01$).

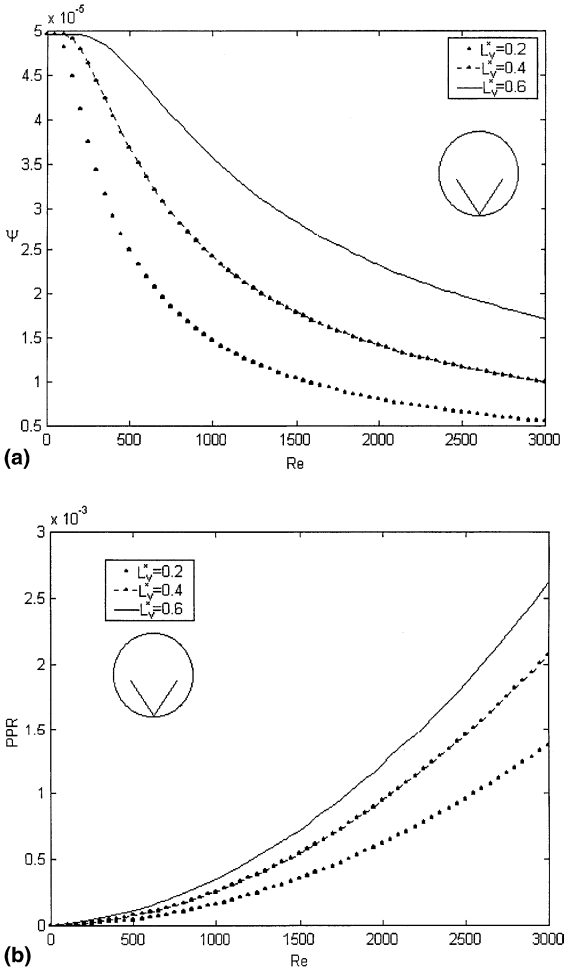

Fig. 10. The effect of fin length on (a) entropy generation and (b) pumping power ratio (V-shaped fin, $\phi = 70°$ and $\tau = 0.01$).

as the Reynolds number is increased, the dimensionless entropy generation values decrease.

As the angle of fin is increased pumping power to heat transfer ratio values decrease (Fig. 9b). For a fixed fin angle pumping power ratio increases with increase of Reynolds number. As seen in the figure pumping power ratio values for angle of 80° and 60° are approaching each other. Because mean Nusselt number values for this two angle case are closer to each other as indicated in Table 4.

Fig. 10a and b are given to show the effect of dimensionless fin length on dimensionless entropy generation and pumping power ratio. In these figures, the value of fin angle is fixed at $\phi = 70°$. Similar trend is observed as explained for previous configurations. That is, as the fin length is increased dimensionless entropy generation values increase (Fig. 10a). As the dimensionless length of fin is increased, pumping power ratio values decrease (Fig. 10b). For a fixed L^* value pumping power ratio increases with increase of Reynolds number.

The effect of dimensionless temperature difference on dimensionless entropy generation and pumping power ratio is given in Fig. 11a and b. Similar effects are observed as indicated in the previous two configurations.

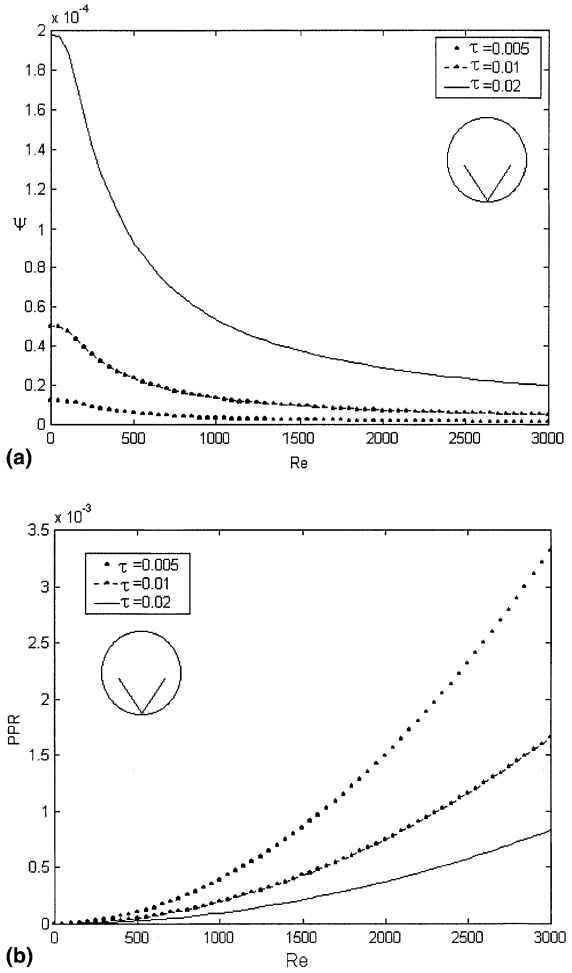

Fig. 11. The effect of dimensionless temperature difference on (a) entropy generation and (b) pumping power ratio (V-shaped fin, $\phi = 50°$ and $L/L_{max} = 0.4$).

5. Conclusions

An entropy generation analysis through a circular duct with three different shaped longitudinal fins for laminar flow was conducted. The following conclusions can be drawn from the present study:

1. In general, as the Reynolds number is increased, the entropy generation decreases and the pumping power to heat transfer ratio increases in all the cases considered. However, as the inlet to wall temperature difference increases, the entropy generation increases and the pumping power to heat transfer ratio decreases in all the cases considered.
2. As the number of thin or triangular fins is increased, the dimensionless entropy generation increases. For higher values of the Reynolds number, the entropy generation for thin fins becomes superior to that corresponding to triangular fins. However, pumping power ratio values for thin fins is higher than that for triangular fins.
3. For all the cases considered, as the length of the fins is increased, the dimensionless entropy generation and the pumping power to heat transfer ratio increase and they depend on dimensionless fin length values.
4. As the fin angle is increased, both the entropy generation and the pumping power to heat transfer ratio increase in the case of triangular fins. For the case of V-shaped fins, the increase of the fin angle causes the increase in both the entropy generation and the pumping power to heat transfer ratio.
5. It is not convenient which shape of the fins is preferable because various demanding in engineering applications. Further, an optimization may be useful but it is out of the scope of this paper.
6. It can be said that entropy generation analyses becomes more superior to traditional CFD analyses and this trend is gradually growing especially in the design of thermodynamics systems.

References

[1] A. Bejan, Entropy Generation through Heat and Fluid Flow, John Wiley & Sons, 1994.

[2] W.M. Kays, A.L. London, Compact Heat Exchanger, McGraw-Hill, New York, 1964.
[3] W.M. Kays, Convective Heat and Mass Transfer, McGraw-Hill, New York, 1964.
[4] R.K. Shah, A.L. London, Laminar Flow Forced Convection in Ducts, Academic Press, 1978.
[5] A.P. Fraas, Heat Exchanger Design, second ed., John Wiley & Sons, 1989.
[6] A. Bejan, The concept of irreversibility in heat exchanger design: counterflow heat exchangers for gas-to-gas applications, J. Heat Transfer 99 (1977) 374–380.
[7] A. Bejan, A study of entropy generation in fundamental convective heat transfer, J. Heat Transfer 101 (1979) 718–725.
[8] A.Z. Sahin, A second law comparison for optimum shape of duct subjected to constant wall temperature and laminar flow, Heat Mass Transfer 33 (1998) 425–430.
[9] P.K. Nag, P. Mukherjee, Thermodynamic optimization of convective heat transfer through a duct with constant wall temperature, Int. J. Heat Mass Transfer 30 (1987) 401–405.
[10] A.Z. Sahin, Irreversibilities in various duct geometries with constant wall heat flux and laminar flow, Energy 23 (1998) 465–473.
[11] G. Fabbri, Optimum performances of longitudinal convective fins with symmetrical and asymmetrical profiles, Int. J. Heat Fluid Flow 20 (1999) 634–641.
[12] G. Fabbri, Optimum profiles for asymmetrical longitudinal fins in cylindrical ducts, Int. J. Heat Mass Transfer 42 (1999) 511–523.
[13] G. Fabbri, Heat transfer optimization in internally finned tubes under laminar flow conditions, Int. J. Heat Mass Transfer 41 (1998) 1243–1253.
[14] I. Alam, P.S. Ghosdastidar, A study of heat transfer effectiveness of circular tubes with internal longitudinal fins having tapered lateral profiles, Int. J. Heat Mass Transfer 45 (2002) 1371–1376.
[15] C.V.M. Braga, F.E.M. Saboya, Turbulent heat transfer, pressure drop and fin efficiency in annular regions with continuous longitudinal rectangular fins, Exp. Thermal Fluid Sci. 20 (1999) 55–65.
[16] R. Kumar, Three-dimensional natural convective flow in a vertical annulus with longitudinal fins, Int. J. Heat Mass Transfer 40 (1997) 3323–3334.
[17] O. Zeitoun, A.S. Hegazy, Heat transfer for laminar flow in internally finned pipes with different fin heights and uniform wall temperature, Heat Mass Transfer (2003).
[18] B. Yu, J.H. Nie, Q.W. Wang, W.Q. Tao, Experimental study on the pressure drop and heat transfer characteristics of tubes with internal wave-like longitudinal fins, Heat Mass Transfer 35 (1999) 65–73.
[19] A. Campo, J. Chang, Correlation equations for friction factors and convective coefficients in tubes containing bundles of internal, longitudinal fins, Heat Mass Transfer 33 (1997) 225–232.
[20] H.F. Oztop, A.Z. Sahin, I. Dagtekin, Entropy generation through hexagonal cross-sectional duct for constant wall temperature in laminar flow, Int. J. Energy Res. 28 (2004) 725–737.